euspen's 25th International Conference & Exhibition, Zaragoza, ES, June 2025
www.euspen.eu

# Negative stiffness module for a highly sensitive low noise seismometer

Sebastiaan Thaens[1], Jan de Jong[1], Dannis Brouwer[1],
Niels van Giessen[2], Jaap Oudes[2], Hans d'Achard van Enschut[2]

[1]*University Twente*
[2]*Settels Savenije GoC*

*Hans.d.Achard@STTLS.nl*

**Abstract**
Active vibration isolation systems rely on a true and low noise reference signal. For Einstein Telescope the lower limit of detection of vibrations needs to be reduced as far as possible, both in amplitude as in frequency. Our work is aimed at a seismometer that measures the displacement of an inertial mass, suspended with low stiffness. To achieve a low enough effective stiffness, the stiffness of the suspension is compensated by a kinematically defined mechanism.
A negative stiffness module is designed and built to realize a floating mass with a decoupling frequency as low as 200 mHz.
A stiffness-compensation of 1000 N/m is created, and an overall system stiffness of 2 N/m is realized.

Seismometer, low noise, sensitivity, negative stiffness, stiffness compensation, buckling, flexures, vibration isolation, kinematic, Einstein Telescope

## 1. Introduction

Active vibration isolation is a key function in high precision equipment; Both in research instrumentation like the Einstein telescope and electron microscopes, as in industrial equipment like nano-lithography. These active isolation modules require a clean reference signal, "a silent reference" to actively decouple the instrument from floor vibrations. The trend in isolation performance is in two directions: Lower decoupling frequency and higher sensitivity (towards lower limit of detection).

The Einstein Telescope requirements are currently the most stringent and commercially available seismometers are not meeting these specifications. Sensitivity will have to be sub-nanometer displacement and lowest detectable frequency should be lower than 250mHz [1,2]. The main purpose and performance of commercially available seismometers is aimed at seismology and geologic exploration; These instruments are optimized for a high dynamic range, and the noise performance needs to be just good enough to resolve seismic background. A quantitative modelling of the seismic background noise is given in [3]. A comprehensive overview of performance benchmark of state of the art seismometers is given in [4]. Einstein Telescope however will only be used when there is no severe seismic activity, and the noise performance needs to be as good as possible. The active floor isolation is the first step in a chain of vibration isolators, it forms the base for a sequence of passive isolation stages.

For a true and sensitive measurement system, noise, hysteresis and non-linearity must be avoided or minimized. Any artefacts included in this reference signal will result in the introduction of undesired movement in the active vibration isolation platform. Once introduced, these artefacts cannot be removed, and can only be suppressed by the passive stages.

The module described in this work is combined with a gravity compensation and a long-stroke 1 DoF guide to create a vertical seismometer function.

In this paper we describe the instrument concept of a high sensitivity, low noise seismometer. In chapter 2 we describe the concepts and the kinematics of the core modules: the 1DoF guide and the stiffness compensation module. The dimensioning will be discussed in chapter 3. Followed by a verification measurement by means of a Proof of Principle set-up in chapter 4.

## 2. Design considerations and Concept selection

Seismometers rely on the principle of inertia for generating the signal. When an inertial mass can be considered to be free floating in space, the displacement as function of time can be measured between the mass and the environment; With low intrinsic noise and drift. In the current set-up we envision to measure displacements by optical means. This has a performance potential down to 20pm RMS. [5].

Vibrations present themselves in 6 directions and in order to counter these all 6 need to be measured. In this work the measurement of vertical vibrations is chosen (z-direction). The force and the direction of gravity is along the measurement direction and needs to be compensated in order to realize a floating mass. To isolate the movements in the chosen direction, a 1 degree of freedom (1DoF) guide needs to be established, with minimize crosstalk between the other measurement directions. This means high stiffness in the direction perpendicular to the movement, whereas in the movement direction the stiffness should be a low as possible.

Together with the mass, this stiffness determines the de-coupling frequency. Below this frequency the mass will follow the environment, above this frequency the environment moves without causing movement of the mass.

A dominant requirement that needs mentioning here is that most seismomenters have an active feedback force, that keeps the floating mass in a "zero"position. In these instruments the needed actuation force is a direct measure of the acceleration of the environment. These feedback systems suffer from drift and electronic noise. To avoid electronic noise the choice in this

work is made for a passive system. Due to the low overall stiffness this implies a high excursion. For practical reasons, this excursion was capped at 1 mm max, which determines the upper limit of the dynamic range. This decision imposes stringent demands on linearity of the force vs excursion (ie the stiffness)

### *2.1. Stiffness compensation*

To reach a low decoupling frequency the stiffness of the 1DoF guide need to be reduced in the movement direction, this is limited by requirements to avoid the crosstalk. This 1DoF guide will be reported separately and is briefly described in section 2.2. To meet the low frequency requirements, the resulting stiffness needs to be compensated by a 'negative'-stiffness.

There are many mechanisms known to create negative stiffness, like for instance bucking of leafsprings or balancing two compression springs in opposite direction [6]. The resulting lateral low stiffness of these solutions is ill defined, due to the freedom in bending shape of the buckling. As discussed earlier, the application of active vibration isolation needs a true, symmetrical and predictable stiffness. This leads to the search for a fully kinematically defined mechanism to compensate the stiffness in the z-direction.

Due to its well defined behaviour and tunability, the concept of choice is a preloaded bi-stable system, which is rendered schematically in below graph (figure 1). In this mechanism, the stiffness is adjustable by the magnitude of the compensation force $\boldsymbol{F_k}$. All joints are chosen to be cross flexure joints, in order to avoid play, friction and hysteresis.

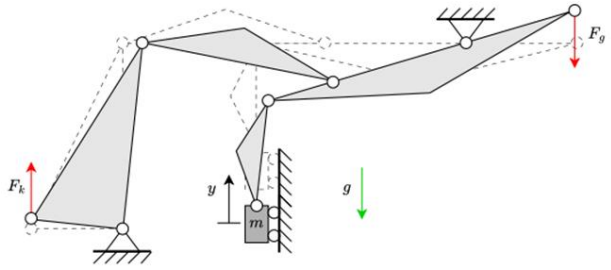


**Figure 1.**
*Conceptual model of the Stiffness and Gravity compensation module. Please keep in mind that the force of gravity is acting on the mass m, and that the mass m is suspended by a 1 DoF guide (not in this figure) with a resulting stiffness of ca 1000 N/m*

A further design decision is to use the cross flexures under a tensile-load, in order to avoid undefined buckling of these flexures when under compression-load. All with the aim of reducing non linear behavior as much as possible. A schematic rendering of this configuration is given in figure 2.

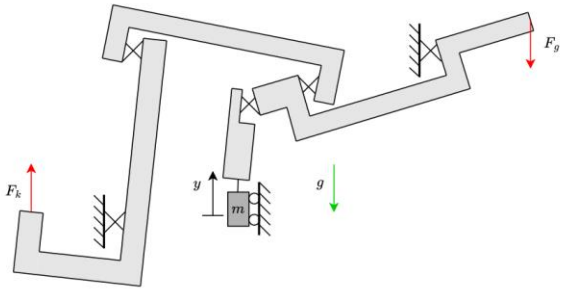


**Figure 2.**
*Conceptual model of the Stiffness and Gravity compensation module. All joints are chosen to be crossflexure joints under tensile-load. Please keep in mind that the force of gravity is acting on the mass m, and that the mass m is suspended by a 1 DoF guide (not in this figure) with a resulting stiffness of ca 1000 N/m*

### *2.2. One Degree of Freedom guide*

The primary function of the 1 DoF guide is to allow only movement in the measurement direction; and with that, block any transfer of energy coming from other directions. For this a construction with 6 folded leafsprings is selected, which ensures symmetry, crosstalk minimization, no friction, play, and low hysteresis. Special attention is given to the large excursion while maintaining linearity and up-down symmetry. The design and verification of this module will be reported separately [7]. A choice was made to set the value of the floating mass to 1 kg. The resulting stiffness in the z-direction of the 1DoF guide is designed to be 1000 N/m. The calculated force vs excursion of the 1DoF guide is plotted in figure 3. The (non-linear FEM) calculation shows that the maximum deviation of the stiffness over the range is as low as 20ppm (edge to center).

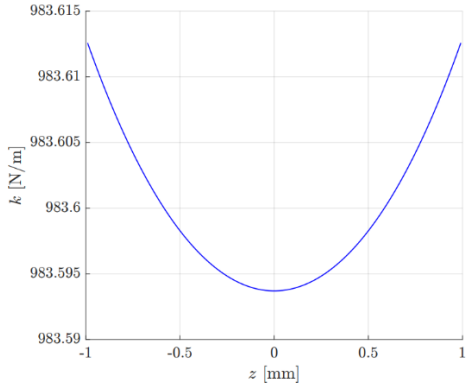


**Figure 3.** *The simulated force-excursion curve for the 1 DoF guide, taken from [7]*

## 3. Dimensioning and detailed design

In a detailed analysis of the conceptual model, the kinematics and force balance study was performed with the use of SPACAR (SPACAR is a flexible multibody dynamics software package, for fast and efficient equilibrium calculations of flexure-based mechanisms.) [8]

In comparison also a Pseudo Rigid Body Model calculation (PRBM) is used [9]. In this Pseudo Ridgid Body Model, flexible segments are modelled as rigid links connected to revolute joints with torsional springs.

The asymmetry in the geometry causes a 1st order non-linearity when the arms flex up or down. The naming of components is shown in figure 4

It can be shown from energy considerations that the 1st order non-linearity can be eliminated when the condition in equation (1) is fulfilled:

$$\frac{c_5}{c_2} = \frac{d}{b}\frac{L_1 + L_2}{L_3}\left(\frac{L_1}{L_2}\right)^2 \qquad \textbf{(1)}$$

(Definition of the parameters are given in figure 4. Stiffness $c_i$ in [N/m]; Lengths $L_i$, b and d in [m] ; Vertical displacement $y$ in [m])

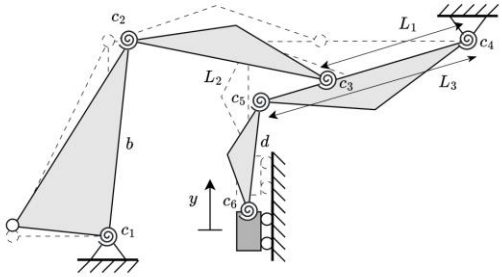


**Figure 4.** *Stiffness compensation module with torsional stiffness components and relevant dimensions defined.*

When the conditions of equation (1) are met, the resulting "negative"-stiffness $\boldsymbol{k}$ is derived, and given in equation (2)

$$k = -k_k u_k \frac{a}{b}\left(\frac{L_1}{L_3^2} + \frac{L_1^2}{L_2 L_3^2}\right) \qquad \textbf{(2)}$$

In this equation the preload force $\boldsymbol{F_k}$ is represented by the stiffness $\boldsymbol{k_k}$ and excursion $\boldsymbol{u_k}$ of a preload spring.

With the detailed dimensioning mentioned in chapter 4, the resulting force and stiffness are calculated with SPACAR and PRBM. Figure 5 plots the force and stiffness over the deflection range. As a comparison a PRBM calculation is added with a slightly higher value of the compensation stiffness. Figure 5B shows that the general agreement between these calculations is fair, considering the independence of the calculation methods; And considering the fact that the resulting stiffness is the subtraction of two large numbers.

For the use as a vertical (z-direction) seismometer a gravity compensation is added, by means of a spring.

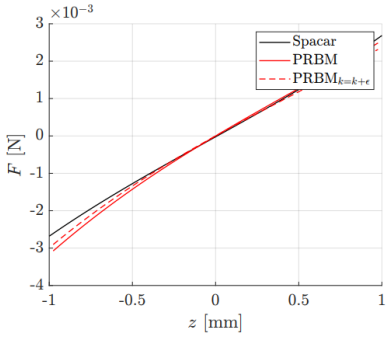


(A) Force over deflection

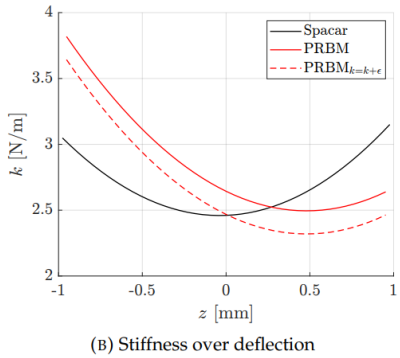


(B) Stiffness over deflection

**Figure 5.** *The force-excursion curve (A) for the total system with the compensation force applied. And the resulting stiffness (B) as function of the excursion*

## 4. Proof of Principle verification

To validate of the models and to demonstrate the kinematics, a Proof of Principle set-up was made (see the photograph in figure 6). The actual dimensioning and design were worked out, based on pragmatic choices on weight and size. As mentioned earlier, a basic (arbitrary) choice of a floating mass of 1 kg was made. To reduce cost and lead-times the crossed leafspring hinges were made out of separate laser cut sheetmetal. Same as the arms of the mechanism. In a later stage the hinges would preferably be made monolythic (by EDM), to reduce creep and hysteresis.

The resulting dimensioning led to:

$L_1 = 70\ mm\ ,\ L_2 = 70\ mm\quad and\quad L_3 = 101.7\ mm$

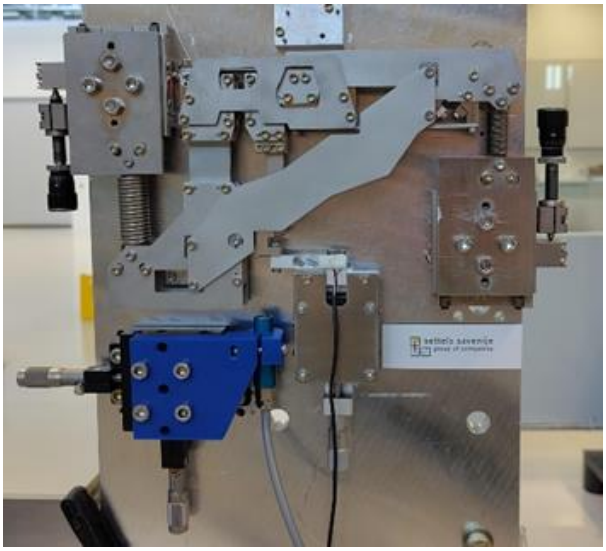

**Figure 6.** *The Proof of Principle set-up*

Both the compensation forces (stiffness and gravity) were generated by springs and made adjustable by a precision spindle. The resulting force was measured by a load-cell, placed at the location where the floating mass would be. The displacement was measured by a laser distance meter, which is described in: [10].

At a fixed pre-load and fixed gravity compensation setting, the position of the load-cell was varied and the resulting force was registered. The measured graph is shown in figure 7

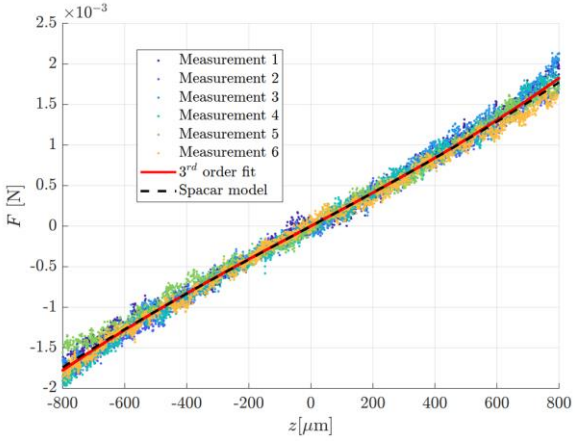


**Figure 7.** *The measured force-displacement of the 'Negative-stiffness'module under realistic load. In red the 3$^{rd}$ order polynomial fit of the data and dashed the SPACAR calculations.*

From a 3$^{rd}$ order polynomial fit to the data in figure 7, an estimation of the stiffness as function of displacement is made by taking the derivative of this fit. This result is plotted in figure

8, together with the predicted values from the SPACAR model. A good qualitative and fair quantitative agreement is demonstrated. A detailed study of the rootcause of this quantitative discrepancy is on-going, in combination with the modelling differences shown in figure 5. Noted is that the 1st order non-linearity is absent or minimal within the measurement accuracy (as designed). This means that the selected dimensions indeed fulfil the condition of equation (1).

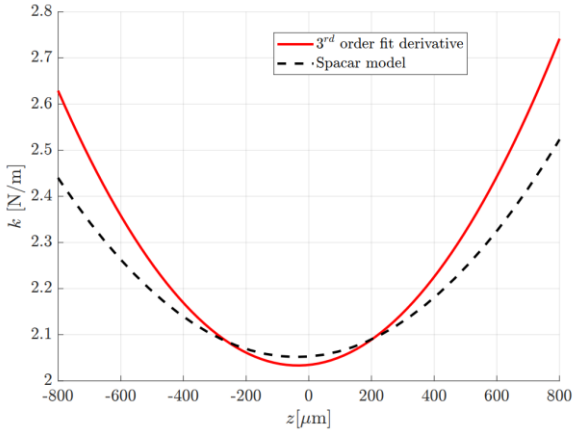


**Figure 8.** *The measured (red) and the calculated (dashed) values of the resulting stiffness after compensating stiffness and effects of gravity.*

An important conclusion from the result in figure 8 is that the overall stiffness seen by the floating mass can be as low as 2 N/m. This means that with a mass of 1kg a decoupling frequency can be reached of 225mHz. This is fulfilling the design target mentioned in chapter 1.

Next the range of adjustability of the 'negative-stiffness' was investigated. In figure 9 the resulting compensation forces are measured at various pre-loads. From this graph it is concluded that the design target of -1000N/m has been realized, with a linear behavior over +/- 1mm excursion.

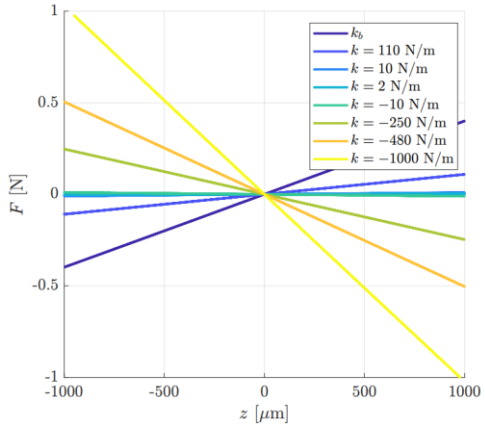


**Figure 9.** *The measured 'negative-stiffness' at various preloads.*

## 5. Conclusions

Summarizing, in this paper we have described the design targets, the design considerations, the concept selection, dimensioning and the measurements on a proof of principle set-up. In chapter 2 we have shown that a fully kinematicaly defined mechanism for stiffness compensation is possible. And we have shown in chapter 4 that the stiffness compensation module can reduce the overall stiffness from 1000N/m to 2N/m. With this a decoupling frequency for a floating mass seismometer of 225mHz can be realised. We have shown that the behavior of the mechanism is adjustable, symmetrical and linear.

We conclude that a highly sensitive seismometer can be built with the described mechanism, when combined with a suitable 1 DoF guide and a sensitive displacement sensor. This will result in a seismometer that will improve the active vibration isolation stages of for instance the Einstein Telescope. The solution that we have shown is scalable and applicable to other applications and performance ranges.

Further work will include the detailed investigation on hysteresis and (temperature) drift, for this the cross flexure hinges will have to be replaced by monolytic hinges, produced by EDM methods. Next will be the integration of the described module with a suitable 1DoF-guide, a mass and a displacement sensor to demonstrate the seismometer functionality.

**Acknowledgements**

The authors wish to thank University Twente and Settels Savenije group of companies for their support. Components were manufactured by Settels Savenije Precision Parts. This work received no external funding. This is original work and all external sources of information and knowhow are listed in the references.

## 6. References

[1] Pushing towards the ET sensitivity using 'conventional' technology Stefan Hild, Simon Chelkowski and Andreas Freise, arXiv:0810.0604 **[gr-qc] (2008)** https://doi.org/10.48550/arXiv.0810.0604

[2] ET-design document : Design Report Update 2020 for Einstein Telescope: https://gwic.ligo.org/3Gsubcomm/docs/ET-0007B-20_ETDesignReportUpdate2020.pdf

[3] Peterson, J. Observations and modeling of seismic background noise. In Open-File Report 93–322; U.S. Geological Survey: Albuquerque, NM, USA, 1993; p. 95.

[4] Kaiming Wang, Wenyi Li, Lijun Zhao, Daxin Yu, and Shaogang Wei. Research on Self-Noise Characteristics of Nine Types of Seismometers Obtained by PDF Representation Using Continuous Seismic Data from the Malingshan Seismic Station, China. *Sensors*, 2023, **23**(1):110. https://doi.org/10.3390/s23010110

[5] Physik Instrumente (PI) SE Co. KG. PIOne Optical Nanometrology Encoder — physikinstrumente.com. https://www.physikinstrumente.com/en/expertise/technology/sensor-technologies/pione-encoder.

[6] J.van Eijk. On the design of plate-spring mechanisms. PhD thesis, University of Technology Delft, 1985
M.P.Koster. Construction principles. Lecture notes WA-163. University Twente. 1993
W.van den Hoek. Lecture notes 4.007.1, University of Technology Eindhoven 1965 - 1984

[7] 1 Dof guide. D van Inzen (2025) Fontys University of Applied Science. Eindhoven

[8] J. B. Jonker and J. P. Meijaard, SPACAR — computer program for dynamic analysis of flexible spatial mechanisms and manipulators. Berlin, Heidelberg: Springer Berlin Heidelberg, 1990, pp. 123–143. SPACAR Project. Spacar wiki, n.d. Accessed: 2024-12-20. https://www. spacar.nl/wiki/doku.php

[9] L.L. Howell, Compliant mechanisms, Wiley-Interscience, 2001. John Wiley & Sons, 2001; ISBN 047138478X, 9780471384786

[10] PI-D-780 Laser-based Optical Sensor: https://www.physikinstrumente.nl/fileadmin/user_upload/pi_benelux/files/Datasheet-Stystem-for-Contactless-Optical-Distance-Measurement.pdf